Redox Processes between NiO and Ni(0) on Carbon for Application to Conversion Battery

Takuya Tsuji[1], Yusaku Yamamoto[1], Hirona Yamagishi[2], Misaki Katayama[1,2], and Yasuhiro Inada[1]

1) *Department of Applied Chemistry, College of Life Sciences, Ritsumeikan University, 1-1-1 Noji-Higashi, Kusatsu 525-8577, Japan*
2) *The SR Center, Ritsumeikan University, 1-1-1 Noji-Higashi, Kusatsu 525-8577, Japan*

Conversion reaction for NiO nanoparticles supported on acetylene black (AB) was analyzed using an *in situ* XAFS technique. The NiO particle supported on AB was synthesized by the impregnation method. For the first discharge process for a test cell of an NiO/AB cathode with a Li anode, it was revealed that the reactions of the Ni species proceeded at two different potentials. This indicates that the reactions in the surface layer and the bulk of the NiO particle have different reduction potentials. In addition, it was clarified that the Ni particles became smaller after the first discharge process and the fine size was kept in the following cycles.

1. Introduction

Graphite is generally used as a negative electrode material of lithium ion secondary batteries (LIBs). In a graphite electrode, the insertion/desorption reactions of lithium ions into/from the graphite layer occur during the charge and discharge processes. When the composition of a product is LiC_6, the theoretical capacity of the graphite electrode is 372 mA h g^{-1} [1], and it is a limit of the energy density for the LIB using the graphite electrode. For next-generation LIBs, a negative electrode using a conversion reaction is expected to become important. The conversion reaction is a reaction of a metal oxide such as NiO with Li^+ and electrons to reduce it to the metal species as shown in eq. (1).

$$NiO + 2Li^+ + 2e^- \rightleftarrows Ni + Li_2O \qquad (1)$$

The theoretical capacity of eq. (1) is 718 mA h g^{-1} [2], which is apparently larger than the graphite electrode, and thus its application as the negative electrode of LIB attracts much attention to overcome the energy limit of the present LIBs.

However, the charge and discharge profiles of such LIBs using NiO show a large irreversible capacity at the first cycle, a large potential polarization, and a poor cycle performance, and these properties are problems for its practical use [3]. It has been clarified that the particle size of NiO greatly affects the reversibility of the charge and discharge reactions [4], and that the small NiO particles show higher battery performance [5]. It has also been reported that it is effective to use a carbon material with high flexibility and conductivity as the matrix of the NiO electrode in order to improve the cycle and rate performances [6,7]. It is thus important to reveal the chemical state of the Ni species during the charge and discharge processes to understand the effect of the particle size on the battery performance. Therefore, we synthesized NiO nanoparticles supported on acetylene black (AB) by an impregnation method and applied *in situ* XAFS measurements to the charge and discharge processes for a test cell of an NiO/AB cathode with a Li anode. We aimed to elucidate the reaction mechanisms of the NiO conversion electrode.

2. Experimental

The NiO particles supported on AB were prepared by an impregnation method. The NiO loading was set to 20 wt%. Powder of AB was added in an aqueous solution of $Ni(NO_3)_2 \cdot 6H_2O$, and the mixture was stirred for 1 h at 60 °C. Then it was dried at 70 °C for 72 h and calcined at 300 °C for 2 h in the air. A mixture of the synthesized NiO/AB and a solution of binder polymer (polyvinylidene difluoride, PVdF) were applied on a Cu current collector foil to prepare an NiO/AB electrode sheet. The mass ratio of the composed NiO/AB and PVdF was 6:4. The prepared NiO/AB electrode, two separator sheets, and a Li metal foil were assembled to an Al-laminated cell for the *in situ* XAFS measurements.

The *in situ* XAFS measurements at the Ni K edge were carried out at BL-3 of the SR Center of Ritsumeikan University (Kusatsu) and BL-7C of Photon Factory (KEK, Tsukuba). During the first two discharge-charge cycles, the XAFS measurements at every 50 mA h g^{-1} were repeated. The constant current charge/discharge operations were carried out, while the operation was stopped during the XAFS measurement.

3. Results and Discussion

Figure 1 shows XANES spectra of the NiO/AB electrode before and after the discharge-charge cycles. The initial spectrum corresponds to that of NiO as shown in Fig. 1(a). For the spectra after the first and second cycles, the energy of the absorption edge is consistent to that of NiO, whereas the peak absorbance at the white line of NiO becomes lower and the spectral amplitude after the absorption edge becomes weak. It is considered that the states of the Ni(II) species after

the discharge-charge cycles are different from the initial NiO. The spectral characteristics with the weakened amplitude can imply the refinement of the NiO particles after the discharge-charge cycles. The spectra in Figs. 1(b) and (c) are almost identical, therefore the same Ni(II) species is regenerated at the second cycle.

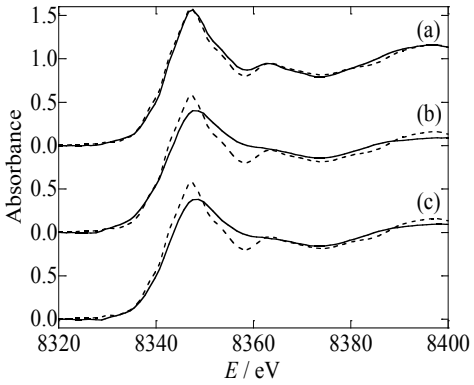

Fig. 1 Comparison of XANES spectra for initial state (a), after first charge (b), and after second charge (c). The dashed lines indicate the spectrum of reference NiO.

XANES spectra after the discharge process were compared with that of Ni foil in Fig. 2. Both spectra after the first and second discharge processes are almost identical, and the edge energies are in agreement with that of Ni(0) foil. On the other hand, the spectra show clear discrepancy from the standard Ni(0) metal, indicating that the formation of a different Ni(0) species from the Ni(0) metal after the lithiation process during the discharge process.

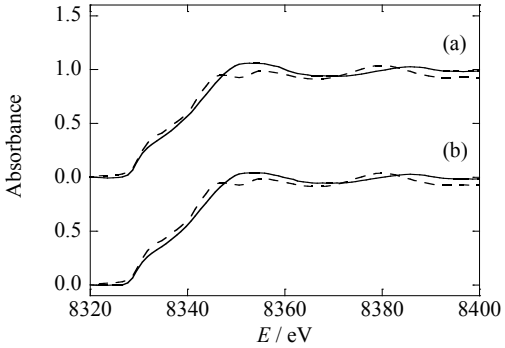

Fig. 2 Comparison of XANES spectra after first (a) and second (b) discharges. The dashed lines indicate the spectrum of Ni foil.

The X-ray absorbance changes at 8348 eV and 8335 eV and the potential profile are shown in Fig. 3 for the first discharge process. The initial species was confirmed as NiO (see Fig. 1), and the NiO species was reduced to the Ni(0) species (see Fig. 2) below 1.0 V vs. Li^+/Li. The spiky behavior seen in Fig. 3(A) was due to the stop of the discharging operation. In Fig. 3(B), the X-ray absorbance at 8348 eV was decreased from 0 mA h g^{-1} to 150 mA h g^{-1} (Region 1). The decrease was terminated in Region 2, where the cell capacity was in the region between 150 mA h g^{-1} and 450 mA h g^{-1}, and the absorbace became almost constant, indicating that the chemical state of the Ni species was not varied. The X-ray absorbance at 8348 eV was again decreased over 450 mA h g^{-1} (Region 3). Since the absorbance was constant over 750 mA h g^{-1}, it was considered that the Ni(II) species was completely reduced in the Regions 1 and 3, where the XANES spectra of the Ni species were changed. On the contrary, in the Regions 2 and 4, the discharge current was assigned to a reaction, where some species except for Ni were reduced.

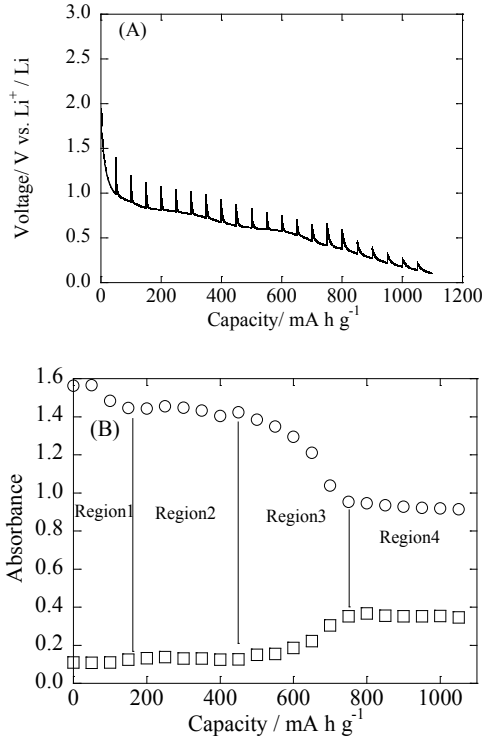

Fig. 3 Potential curve of the first discharge process (A) and the X-ray absorbance changes (B) at 8348 eV (○) and at 8335 eV (□).

The difference spectra before and after the overall first discharge process, before and after Region 1, and before and after Region 3 are compared in Fig. 4. The difference spectra in the Regions 1 and 3 are in agreement with each other, and also are consistent with that for the overall difference at the first discharge process. Therefore, the same reduction reactions occur in both the Regions 1 and 3.

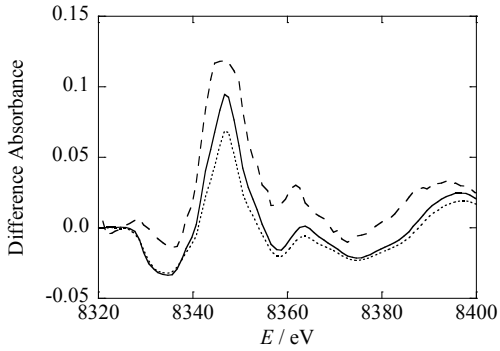

Fig. 4 Difference spectra before and after the overall first discharge process (solid line), and between the start and the end of the Regions 3 (dotted line), 1 (dashed line).

The absorbance changes in Regions 1 and 3 were 21% and 79% of the overall change for the first discharge process, respectively. In this study, the particle size was estimated to be 7 nm on the basis of the peak width of the X-ray diffraction line of NiO. If the thickness of the surface layer is assumed to 3 Å for the spherical NiO particles, the ratio of the Ni species in the surface layer and the remaining bulk region of the particle is calculated to be 23% and 77%, respectively, and these ratios are close to the above ratios of 21% and 79%. Therefore, it is reasonably considered that the NiO species located in the surface layer is reduced in Region 1, and the reduction for the remaining NiO species in the inner region of the particle proceeds in the Region 3. The proportions, 21% for Region 1 and 79% for Region 3, derive the discharge capacity of 30 mA h g^{-1} and 114 mA h g^{-1}, respectively, when the reduction reaction of eq. (1) with the theoretical capacity of 144 mA h g^{-1} is assumed. The experimentally observed capacities in Fig. 3 were 150 mA h g^{-1} and 300 mA h g^{-1}, respectively, and they are 3-5 times larger than the calculated ones. It is considered that these capacities include another reduction process than eq. (1). As an electrode reaction involving Ni and Li^+, the formation reaction of an $NiLi_x$ alloy is the most reliable possibility as given in eq. (2).

$$Ni + xLi^+ + xe^- \rightarrow NiLi_x \qquad (2)$$

Furthermore, the insertion reaction of Li into AB to form LiC_6 also contributes to the total discharge capacity of ca. 1100 mA h g^{-1}.

After the first discharge process, the charge/discharge cycles proceed reversibly. Figure 5 shows the potential curves (A) and the X-ray absorbance at 8348 eV and 8335 eV (B) in the first charge process and the second discharge-charge cycle. In the first charge process, the X-ray absorbance was

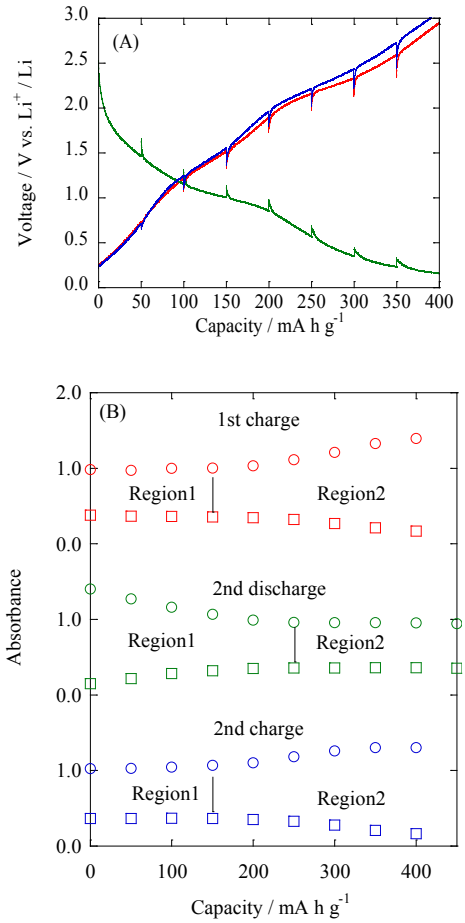

Fig. 5 Potential curves (A) and the X-ray absorbance changes (B) at 8335 eV (○) and 8348 eV (□) in the first charge (red), second discharge (green), and second charge (blue) processes.

unchanged in the capacity region of less than 150 mA h g^{-1} (Region 1), and was changed in the region between 150 and 400 mA h g^{-1} (Region 2). Because the Ni species keeps its chemical state in Region 1, it is considered that the delithiation reaction of AB occurs first in Region 1. As discussed above, the $NiLi_x$ alloy species is reasonably considered to form in the first discharge process. Because the observed capacity (250 mA h g^{-1}) in Region 2 of the first charge process was clearly larger than the theoretical one (144 mA h g^{-1}) for the oxidation from Ni(0) to NiO, it was found that the excess capacity was due to a dealloying reaction as shown in eq. (3) before the formation of NiO. After the dealloying reaction, the formed Ni(0) species is oxidized to NiO in a reaction given by eq. (4), where NiO* denotes the Ni(II) oxide species different from the bulk NiO because of the inconsistent XANES spectra (see Fig. 1).

$$NiLi_x \rightarrow Ni + x\,Li^+ + xe^- \quad (3)$$

$$Ni + Li_2O \rightarrow NiO^* + 2Li^+ + 2e^- \quad (4)$$

In the second discharge process shown in Fig. 5(B), the X-ray absorbance was changed in the capacity region from 0 mA h g^{-1} to 250 mA h g^{-1} (Region 1), and it became constant for the capacity over 250 mA h g^{-1}. The difference from the first discharge in Fig. 3 is that the reaction of the Ni species finishes in Region 1, and that the reduction potential *ca*. 1.0 V is apparently higher than that of Region 3 in the first discharge process in Fig. 3 and is approximately equal to that of Region 1 (reduction in the surface layer). The similarity of the reduction potential of NiO* formed after the first charge process implies that the Ni(II) sites in the NiO* species are equivalent to those in the surface layer of the NiO particle. This consideration is supported by the formation of fine NiO particles as suggested by the difference in the XANES spectra (see Fig. 1). All Ni(II) sites in the fine NiO* particles are regarded to be equivalent, and the redox cycles of the Ni species between NiO* and $NiLi_x$ alloy proceed reversibly in the potential range from 0.5 V to 2.0 V after the refinement of the Ni particles occurred in the first discharge process.

4. Conclusions

In the present study, the NiO particle supported on AB was synthesized, and the chemical state of the Ni species in the NiO/AB electrode during the charge and discharge processes was analyzed using the *in situ* XAFS technique. In the first discharge process, it was clarified that the reactions in the surface and bulk regions of NiO particles occured at different potentials. The observed charge and discharge capacities were larger than the theoretical capacity for the reaction between NiO and Ni. It is considered that the formation of the $NiLi_x$ alloy occurs in the discharge process in addition to the conversion reaction of the Ni species. In addition, the initial NiO particle was not reproduced after the first cycle. It was concluded that the Ni particles became fine after the first discharge process and kept the fine size in the following charge-discharge cycles. These findings are important in promoting researches toward the practical use of the conversion reaction.

Acknowledgement

The XAFS measurements at the Photon Factory (KEK) were performed under the approval of the Photon Factory Program Advisory Committee (Proposal No. 2017G037).

References

[1] I. Lahiri, S. W. Oh, J. Y. Hwang, S. Cho, Y. K. Sun, and R. Banerjee, *ACS Nano*, **2010**, *4*, 3440.

[2] A. Caballero, L. Hernan, J. Morales, Z. Gonzalez, A. J. Sanchez-Herencia, and B. Ferrari, *Energy Fuels*, **2013**, *27*, 5545.

[3] Z. Yao, S. Kim, M. Aykol, Q. Li, J. He, and C. Wolverton, *Chem. Mater.*, **2017**, *29*, 9011.

[4] J.-H. Jang, B.-M. Chae, H.-J. Oh, and Y.-K. Lee, *J. Power Sources*, **2016**, *304*, 189.

[5] P. Poizot, S. Laruelle, S. Grugeon, L. Dupont, and J. M. Tarascon, *Nature*, **2000**, *407*, 496.

[6] X. Liu, S. W. Or, C. Jin, Y. Lv, C. Feng, and Y. Sun, *Carbon*, **2013**, *60*, 215.

[7] Y. Zou and Y. Wang, *Nanoscale*, **2011**, *3*, 2615.